

B. A. R. C./I-341

B. A. R. C./I-341



सत्यमेव जयते

**GOVERNMENT OF INDIA
ATOMIC ENERGY COMMISSION**

A CODE FOR LEAKAGE NEUTRON SPECTRA THROUGH THICK SHIELDS

by

**P. S. Nagarajan, P. Sethulakshmi and C. P. Raghavendran
Division of Radiological Protection**

**BHABHA ATOMIC RESEARCH CENTRE
BOMBAY, INDIA**

1975

B.A.R.C./I-341

B.A.R.C./I-341

GOVERNMENT OF INDIA
ATOMIC ENERGY COMMISSION

A CODE FOR LEAKAGE NEUTRON SPECTRA THROUGH THICK SHIELDS

by

P.S. Nagarajan, P. Sethulakshmi and C.P. Raghavendran
Division of Radiological Protection

BHABHA ATOMIC RESEARCH CENTRE
BOMBAY, INDIA
1975

INIS Subject Category : F51; A31

Descriptors :

INTERMEDIATE NEUTRONS

NEUTRON LEAKAGE

NEUTRON SPECTRA

RADIATION MONITORING

ACCELERATORS

REACTOR COMPONENTS

SHIELDS

COMPUTER CODES

CONCRETES

WATER

SHIELDING MATERIALS

KERMA

ANISOTROPY

ISOTROPY

MONTE CARLO METHOD

MEAN FREE PATH

ABSTRACT

An exponential transform Monte Carlo code has been developed for deep penetration of neutrons and the results of leakage neutron spectra of this code have been compared with those of a basic Monte Carlo code for small thicknesses thus checking the code. This report discusses the development of the code, optimisation of certain transform parameters and presents results for a few thick shields of concrete and water in the context of neutron monitoring in the environs of accelerator and reactor shields.

A CODE FOR LEAKAGE NEUTRON SPECTRA THROUGH THICK SHIELDS*

by

P.S. Nagarajan, P. Sethulakshmi and C.P. Raghavendran

1. INTRODUCTION

The motivation for the development of this code was to get a unique shape of the intermediate energy region of the leakage neutron spectra through thick shields. If such a reliably unique or near-unique shape exists then the conversion factors relating the response of various radiation protection monitors to dose equivalent could be computed whether the monitors are bare or backed by a phantom. This is because thermal and fast neutron monitoring and dose/dose equivalent measurements are relatively satisfactory but not those of the intermediate energy range. However, this work leads to the spectrum over the entire energy range.

2. METHOD

The procedure and the code used in this study were developed by us. The exponential transform method chosen for this purpose is discussed in an excellent review by CLARK¹.

2.1. Theory

The transport equation

$$\vec{\Omega} \cdot \vec{\nabla} \phi(\vec{r}, \vec{\Omega}, E) + \sigma(\vec{r}, E) \phi(\vec{r}, \vec{\Omega}, E) = S(\vec{r}, \vec{\Omega}, E) + \sum_i \iint dE' d\Omega' \phi(\vec{r}, \vec{\Omega}', E') \sigma(\vec{r}, E') [\sigma_i(\vec{r}, E') / \sigma(\vec{r}, E')] \times \alpha_i K_i(\vec{r}; \vec{\Omega}' \rightarrow \vec{\Omega}, E' \rightarrow E) \quad \text{----- (1)}$$

* Part of this work was presented at the First Asian Regional Congress on Radiation Protection, Dec. 15-20, 1974, Trombay, Bombay.

using a transformation

$$\psi(\vec{r}, \vec{\Omega}, E) = \exp[g(\vec{r}, \vec{\Omega}, E)] \cdot \phi(\vec{r}, \vec{\Omega}, E) \quad \text{---(2)}$$

becomes

$$\begin{aligned} & \vec{\Omega} \cdot \vec{\nabla} \psi(\vec{r}, \vec{\Omega}, E) + [\sigma(\vec{r}, E) - \vec{\Omega} \cdot \vec{\nabla} g(\vec{r}, \vec{\Omega}, E)] \psi(\vec{r}, \vec{\Omega}, E) \\ & = S(\vec{r}, \vec{\Omega}, E) + \sum_i \iint dE' d\Omega' \psi(\vec{r}, \vec{\Omega}', E') \times \\ & \quad [\sigma(\vec{r}, E') - \vec{\Omega}' \cdot \vec{\nabla} g(\vec{r}, \vec{\Omega}', E')] \cdot \frac{\sigma(\vec{r}, E)}{\sigma(\vec{r}, \vec{\Omega}, E) - \vec{\Omega} \cdot \vec{\nabla} g(\vec{r}, \vec{\Omega}, E)} \times \end{aligned}$$

$$\alpha_i \cdot \exp[g(\vec{r}, \vec{\Omega}, E) - g(\vec{r}, \vec{\Omega}', E')] \cdot K_i(\vec{r}; \vec{\Omega}' \rightarrow \vec{\Omega}, E' \rightarrow E) \quad \text{---(3)}$$

It is readily seen that (1) and (3) are of the same form. Hence a solution of (3) is obtained by the Monte Carlo method and using (2) solution of (1) is obtained. In our work a form of (2) (only one space dimension)

$$g(\vec{r}, \vec{\Omega}, E) = k \sigma(E) z \quad \text{---(4)}$$

was used where $0 < k < 1$ and $\sigma(E)$ is the total macroscopic cross section.

A transform Monte Carlo code was written and was checked against a basic Monte Carlo code for small thicknesses of a water slab. The agreement was good thus checking the reliability of the code. Varying k , for a given thickness we arrived at the same results (within statistical spread) thus checking the internal self consistency of the code.

2.2. Choice of k

For a given source energy and slab thickness and slab material, there is a small range of optimum values of k . However, there is no

simple or direct way of finding this. Hence considerable effort was put in to work-out a rationale for the selection of k for large thicknesses since the variance is related to k in an involved manner. If k is too small the benefit of the transformation is lost. On the other hand if it is too close to unity the particles are forced to leak out too soon i.e. without having had enough collisions to slow down thus causing a large variance in the low energy part of the spectrum. However, it should be remembered that in the method there is no approximation involved but the problem in practice is to get results within acceptable spread for reasonable number of particle histories or computational effort.

An exploratory study was made for a simplified system. For a few values of scattering probability $P_s = \frac{\sigma_s}{\sigma}$ and for a number of values of k and for thicknesses n/σ , for $n = 10, 20, 30$ the transmission was computed. (In each computation P_s is kept constant for all collisions and this corresponds to one large energy group in a multigroup approach). Based on the variance of the results the right value of k could be chosen. In this study the transformation $g(\vec{r}, \Omega, E)$ was only $k\sigma(E)$, and $\sigma(E)$ was kept a constant equal to 1 cm^{-1} . Table 1 shows the 'best' values of k for two values of P_s for thicknesses upto 30 mean free paths. This study yielded some guidance for the real problem. However, it should be admitted that this was not always successful. We still had to have some trial and error approach for the choice of k . Thus this exploratory study was not an unmixed success.

3. A FEW DETAILS IN THE SOLUTION OF EQUATION (3)

3.1. In each run for a given source energy, slab thickness and material 15,000 histories are repeated five times. The time taken for a run in

the RESM-6 computer was about 30 minutes and the actual time depended upon (i) the number of mean free paths of the shield, (ii) the material of the slab, water or concrete, (iii) the transform constant, and (iv) the source energy (0.5 to 14 MeV). Anisotropy (in c.m. system) was considered for all elements for elastic scattering but inelastic scattering was taken to be isotropic in the c.m. system. The composition of the medium is variable and the one used in these test studies is given in table 2.

3.2. Sampling flight distance

The free flight distance (distance between either the source or a collision point and the next collision point) is sampled as

$$d = - \ln R / [\sigma (1 - k \cos \theta)] \quad \text{----- (5)}$$

where θ is the angle between the Z axis and the neutron direction and R is a random number. The cross section data was taken from STEHN et al², SCHMIDT³, PEREY and KINNEY⁴ and KINNEY and PEREY⁵.

3.3 Weightage adjustments

At each collision the weight of the particle is changed from w_1 to w_2 given by

$$w_2 = w_1 \cdot \frac{\sigma_s(E)}{\sigma(E)} \cdot \frac{\exp[kZ(\sigma(E_2) - \sigma(E_1))]}{(1 - k \cos \theta)} \quad \text{---- (6)}$$

where E_1 and E_2 are the energies of the neutron before and after the collision, at the location Z of the collision; θ is the direction of the neutron before collision; and the weight of the particle is unity at source (i.e. $Z = 0$)

All collisions are treated as scattering events with suitable weight adjustments (factor $\frac{\sigma_s}{\sigma}$ in(6)).

3.4. Sampling from K

The anisotropy in the neutron scattering should be taken into account and the shape of the angular distributions vary considerably with energy. If we have a computer of as large a memory as the present day machines, all the angular distribution data or the cumulative (angular) distribution functions could be stored for straight forward sampling. However, as the memory size of the machine available with us is limited, a sampling scheme was developed (NAGARAJAN et al 1974) in which the cosine of the scattering angle is obtained as a double Legendre polynomial summation over a scaled energy variable and a random number^{6,7}. The data used was from GARBER et al⁸ and LANGER et al⁹.

3.5. Scoring

Whenever a particle crosses the boundary of the slab after n th collision an amount of $(W/\cos \theta_n)$ is added to the corresponding energy group where θ_n is the angle between normal to the surface (in our case x axis) and the direction of the neutron. Either 30 or 90 energy groups were used for storage of results depending on the statistics.

4. RESULTS AND DISCUSSION

Figs. 1 through 8 show the computed leakage neutron spectra for 5 and 10 mean free paths in water and concrete, for two scattering laws viz (i) isotropic scattering in the C.M. system and (ii) BNL-400 data⁸. In all the results for concrete and for water the dip between 0.4 and 0.5 MeV is due to the elastic scattering peak (in the 0.4 to 0.5 MeV energy group) of oxygen. The results for all shields are approximately $1/E$ in nature upto

10 MeV, except for 0.3 MeV and 0.5 MeV source energies. The wiggling shapes are all clearly the result of the variations in the cross sections. The elastic scattering cross section curve for oxygen has in addition to the prominent peak between 0.4 and 0.5 MeV, five peaks between 1 and 2 MeV, a deep trough between 2 and 3 MeV, again peaks between 3 and 4 MeV and later on a number of rather large ripples. Corresponding to each peak in the cross section there is a trough in the leakage spectrum and vice versa. Thus the spectra show dips in the 0.4 to 0.5 MeV group, in the 1 and 2 MeV group, and in the 3 and 4 MeV group. To a less extent peaks of Silicon and to a negligible extent peaks of Calcium are responsible for the wiggles in the fast neutron range of the spectrum. Though our immediate interest was in the intermediate energy range the code yields reliable results in the entire energy range. Fig. 9 thro' 12 show leakage spectra for 100 cm - thick concrete and water slabs. These are similar to the earlier figures. The leakage or transmitted neutron kerma values

were calculated as given by

$$T_k(E_0) = \int_{0.1eV}^{E_0} \phi(E) k(E) dE$$

where $k(E)$ is the tissue kerma values for neutrons of energy E , and E_0 is the incident neutron energy.

Values of kerma were taken from Booth and Caswell¹⁰, Caswell et al¹¹, and Dennis¹². Computed values of T_k are presented in table 3 along with those from Schmidt¹³ and Clark et al¹⁴. It is seen that there is better agreement between our results of isotropic scattering law and those of the others. It should of course be remembered that there is bound to be large variations

because of

- (i) differences in compositions used by us and in references 13 and 14, and
- (ii) our method forces neutrons to lower energies (in addition to forcing them to larger depths in space) thus increasing the variance in the MeV region; and the kerma values are large at higher energies thus any agreement may be a matter of chance.

However, as seen in the figures the spectrum in the MeV region is not totally unreliable. But it is not accurate enough for these comparisons.

4.1 Further Program:

The packages developed for this code and the processed neutron cross section data, will be made use of for composite heterogeneous shields. This comprehensive code is under development.

REFERENCES

1. CLARK F.H., Report ORNL-RSIC-14 (1966)
2. STEHN J.R., GOLDBERG M.D., MAGURNO B.A. and WEINER-CHASMAN R.,
Report BNL - 325 (II ed) Supplement No. 2 Vol.1 and 2 (1964).
3. SCHMIDT J.J., Report KFK-120 (EANDC-E-35 U) (1962).
4. PEREY F.G., and KINNEY W.E., Report ORNL-4519 (1970)
5. KINNEY W.E. and PEREY F.G., Report ORNL-4517 (1970)
6. NAGARAJAN P.S., RAGHAVENDRAN C.P., SETHULAKSHMI P., and BHATIA D.P.
A random sampling technique for choosing scattering angles from
arbitrary angular distributions in dosimetric and shielding
computations' - Paper presented at the International Symposium
on 'Radiation Physics', Calcutta (1974).
7. NAGARAJAN P.S., SETHULAKSHMI.P, RAGHAVENDRAN C.P., and BHATIA D.P.,
Report BARC 789 (1975)
8. GARBER D.I., STROMBERG L.G., GOLDBERG M.D., GULLEN D.E., and
MAY V.M., Report BNL-400 (III Edn.) Vol.1 and 2 (1970).
9. LANGER I., SCHMIDT J.J. and WOLL D., Report KFK-750 (1968).
10. BACH R.L. and CASWEL R.S., Radiation Research 35 (1), pp1-25(1968).
11. CASWEL R.S., COYNE J.J. and RANDOLPH M.L. 'Studies of energy
deposition by neutrons', second symposium on 'Neutron Dosimetry in
Biology and Medicine' EURATOM, Neuharberg Sept. 30-Oct.4 (1974).
12. DENNIS J.A., Phys. Med. Biol. 18 (3) pp 379-395 (1973).
13. SCHMIDT F.A.R., Report ORNL-TM-2284 (1968).
14. CLARK F.H., BETZ N.A., and BROWN J. Report ORNL-3926 (1967).

TABLE 1

CHOICE OF THE 'BEST' VALUES OF k

P_n	Thickness in m.f.p.	k
0.5	10	0.80
	20	0.80
	30	0.85
0.9	10	0.3 - 0.4
	20	0.4
	30	0.5

TABLE 2

COMPOSITION OF CONCRETE USED IN THE TEST RUNS

Element	wt%
Oxygen	55.9
Silicon	38.2
Calcium	5.4
Hydrogen	0.5

Table - 1

VALUES OF NEUTRON KERMA TRANSMISSION THROUGH CONCRETE AND WATER

Source neutron energy (MeV)	Anisotropy considered as per BNL-400 (1970)				Isotropy assumed for all elements						From Schmidt (1968) & from Clark et al (1967)		
	Water 100 cm	Concrete			Water 5 λ_0	10 λ_0	100 cm	Water 5 λ_0	10 λ_0	100 cm	Concrete		
		5 λ_0	10 λ_0	100 cm							5 λ_0	10 λ_0	100 cm
14	4.8(-10)	9.0(-8)	6.1(-9)	2.0(-9)	2.9(-8)	4.7(-10)	1.1(-10)	5.6(-8)	2.1(-9)	4.2(-10)	4.0(-8)	1.4(-9)	2.7(-10)
10	1.4(-10)	6.1(-8)	3.1(-9)	1.1(-9)	2.4(-8)	3.4(-10)	6.6(-11)	4.5(-8)	1.3(-9)	5.0(-10)	3.2(-8)	9.0(-10)	3.8(-10)
8	-	-	-	-	-	-	-	-	-	-	4.0(-8)	1.2(-9)	3.5(-10)
7.5	1.0(-10)	7.6(-8)	5.1(-9)	1.8(-9)	2.6(-8)	3.4(-10)	3.7(-11)	5.6(-8)	1.9(-9)	4.9(-10)	-	-	-
6	-	-	-	-	-	-	-	-	-	-	3.5(-8)	1.0(-9)	2.7(-10)
5	4.2(-12)	1.1(-7)	5.0(-9)	2.3(-10)	2.8(-8)	4.4(-10)	5.2(-13)	6.4(-8)	1.3(-9)	1.0(-10)	-	-	-
4	-	-	-	-	-	-	-	-	-	-	2.9(-8)	7.5(-10)	16.3(-11)
2	8.5(-16)	1.0(-7)	1.4(-9)	1.7(-11)	6.8(-8)	1.7(-9)	8.5(-16)	8.0(-8)	1.0(-9)	9.6(-12)	1.5(-8)	1.5(-10)	2.2(-12)
1.3	-	-	-	-	-	-	-	-	-	-	1.2(-8)	1.3(-10)	9.0(-15)
1	-	2.1(-7)	6.8(-9)	-	3.4(-8)	4.7(-10)	-	2.1(-7)	6.8(-9)	-	-	-	-
0.7	-	-	-	-	-	-	-	-	-	-	8.0(-9)	6.0(-11)	1.5(-16)
0.5	-	5.0(-7)	1.0(-7)	-	6.4(-8)	2.7(-9)	-	5.1(-7)	1.0(-7)	-	-	-	-

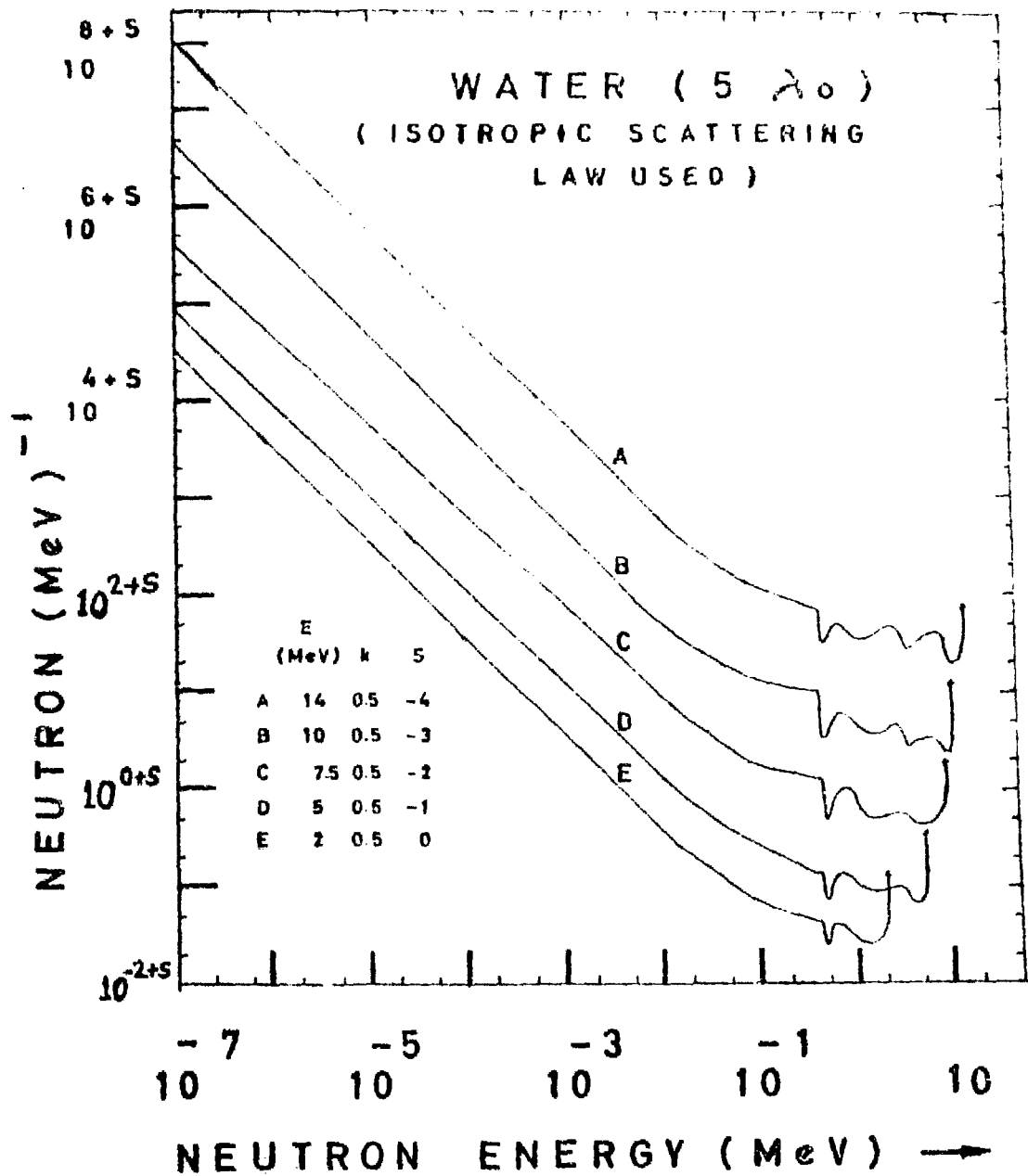


FIG. 1 LEAKAGE NEUTRON SPECTRA THROUGH 5 MEAN FREE PATHS OF WATER

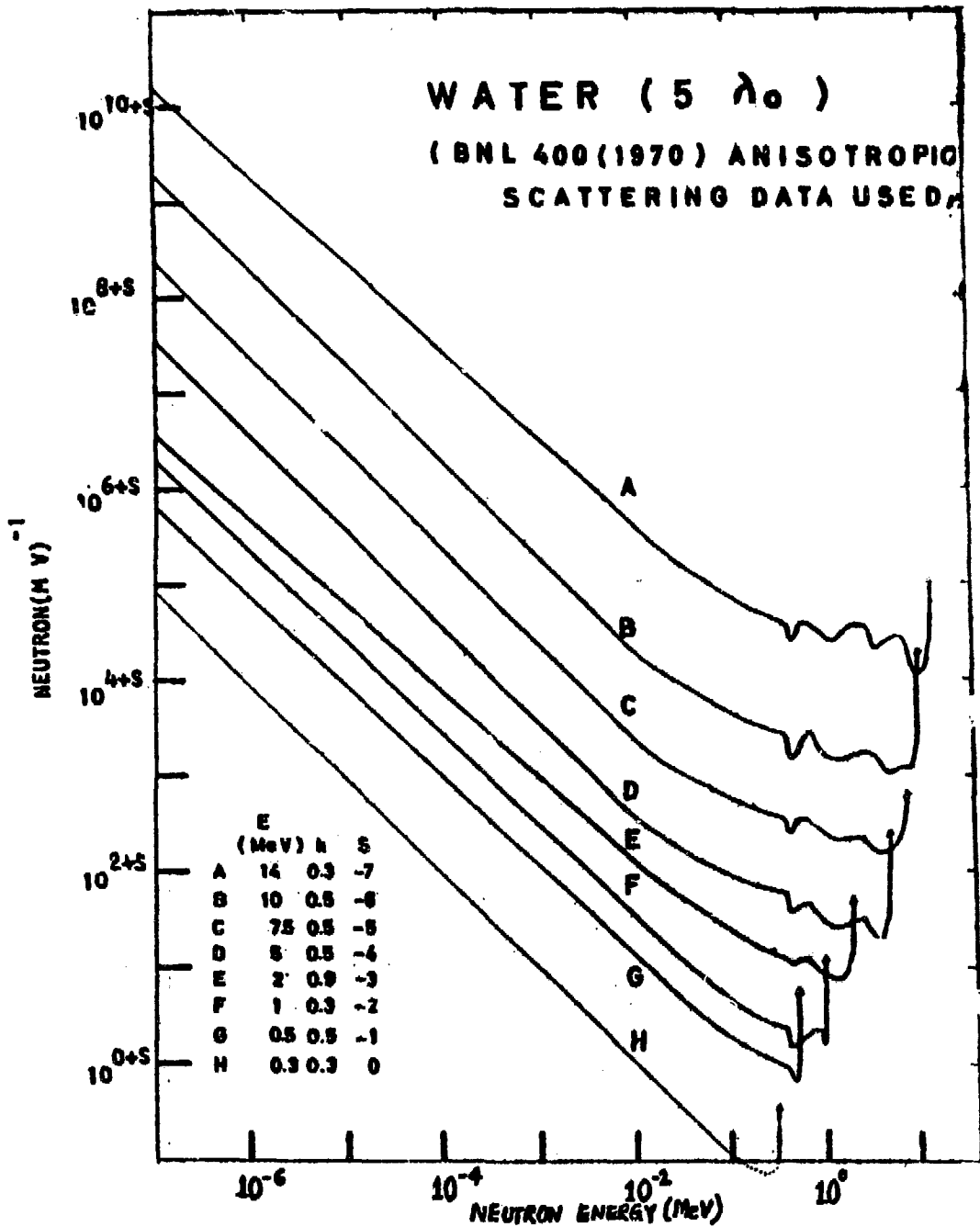


FIG. 2 LEAKAGE NEUTRON SPECTRA THROUGH 5 MEAN FREE PATHS OF WATER

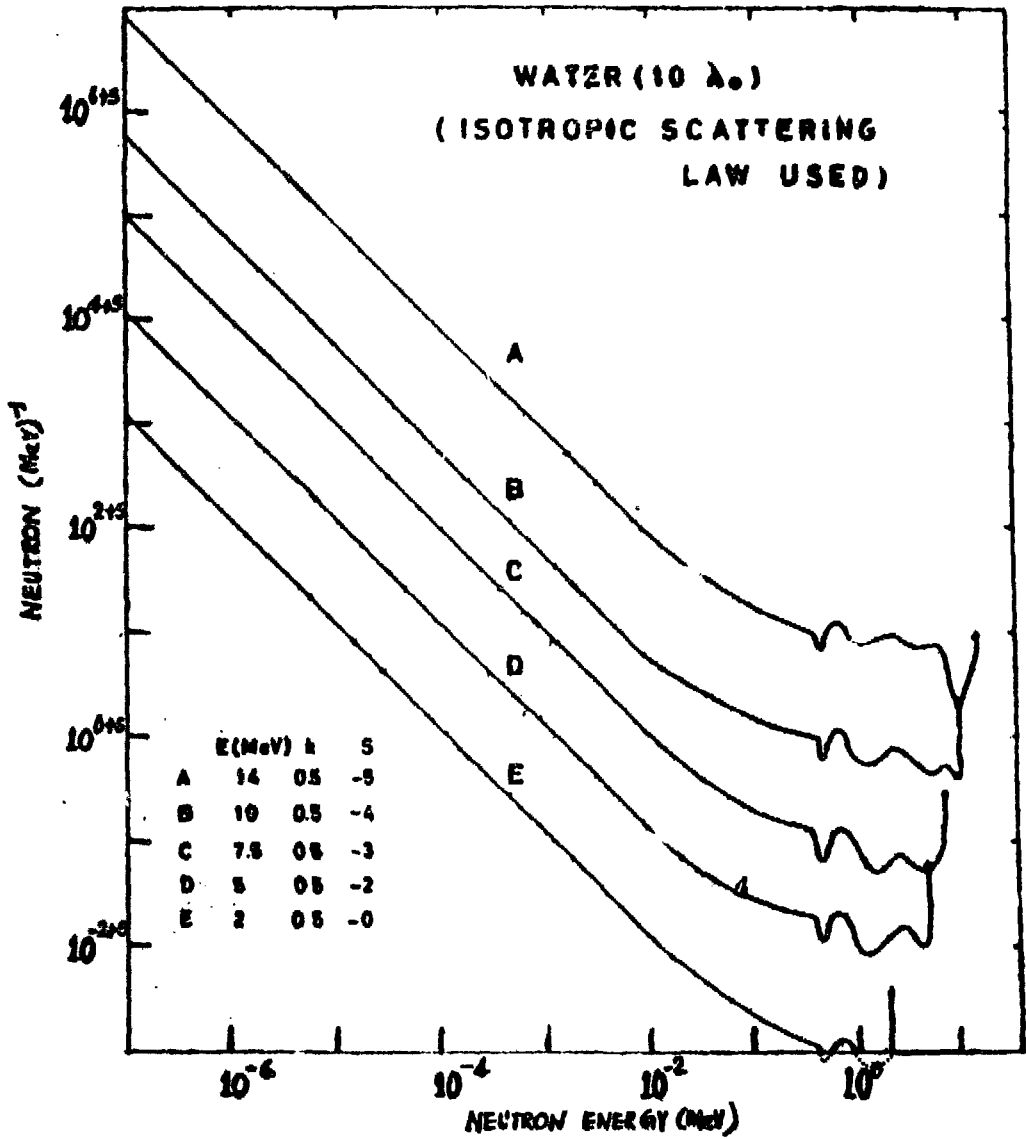


FIG. 3 LEAKAGE NEUTRON SPECTRA THROUGH 10^1 MEAN FREE PATHS OF WATER

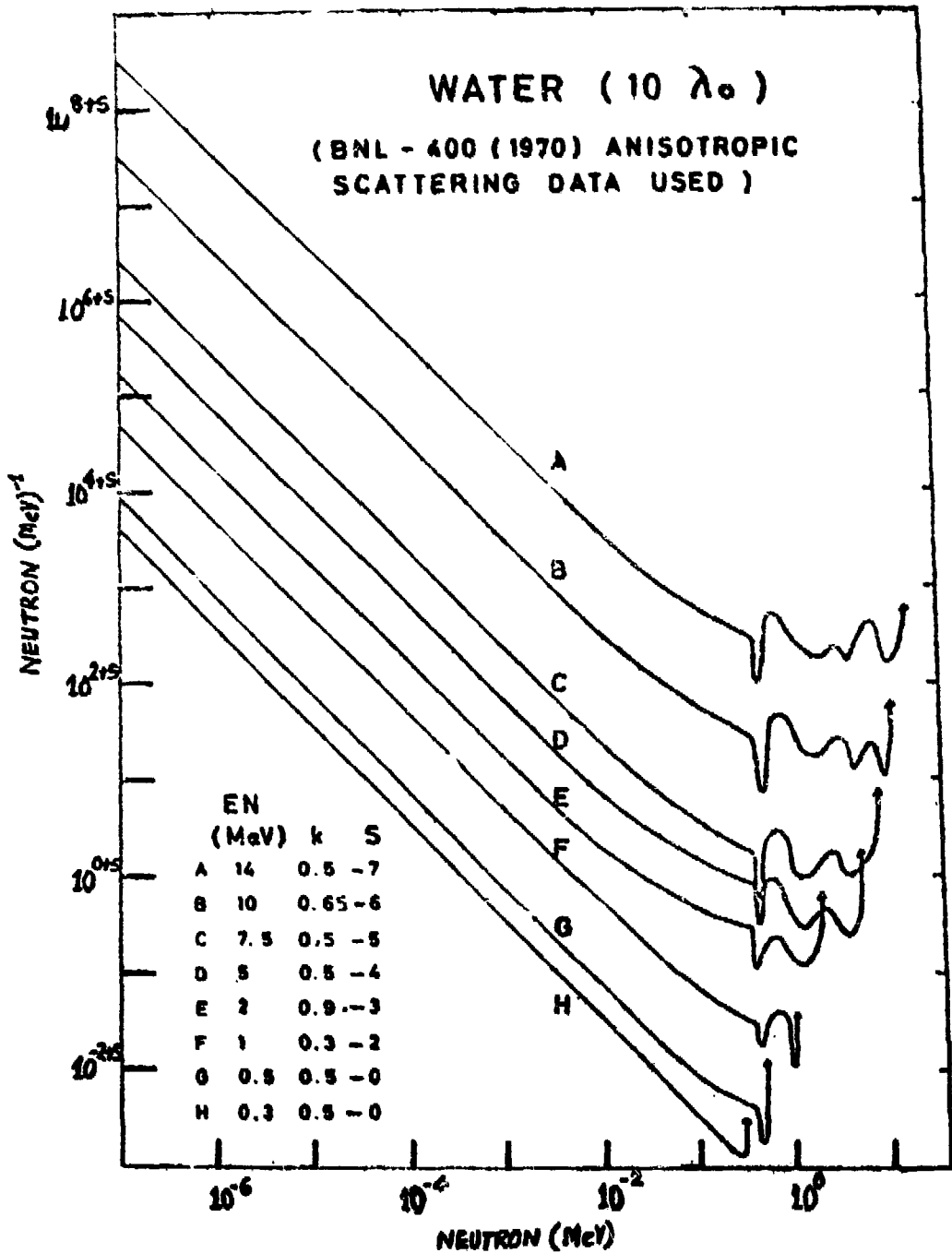


FIG. 4 LEAKAGE NEUTRON SPECTRA THROUGH 10 MEAN FREE PATHS OF WATER

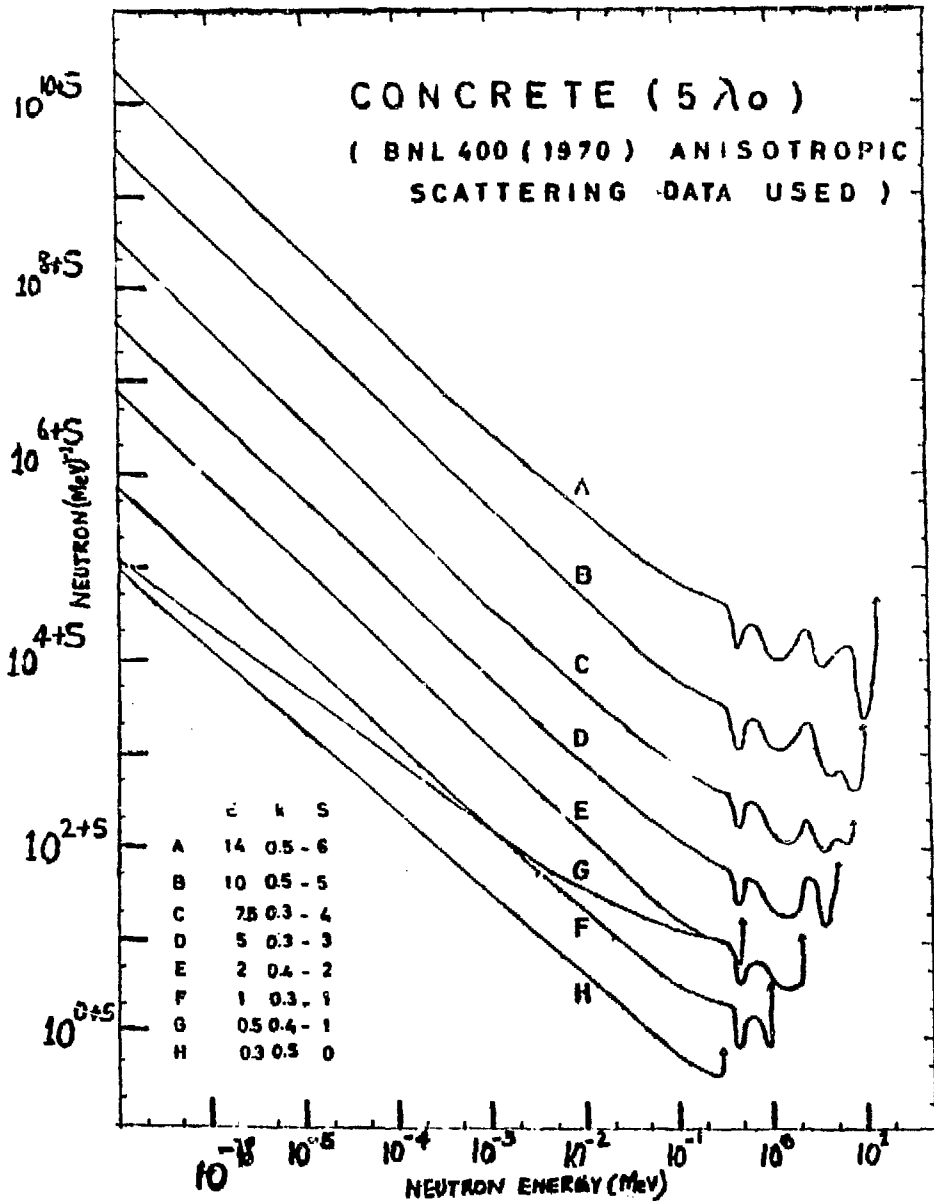


FIG. 6 LEAKAGE NEUTRON SPECTRA THROUGH 5 MEAN FREE PATHS OF CONCRETE

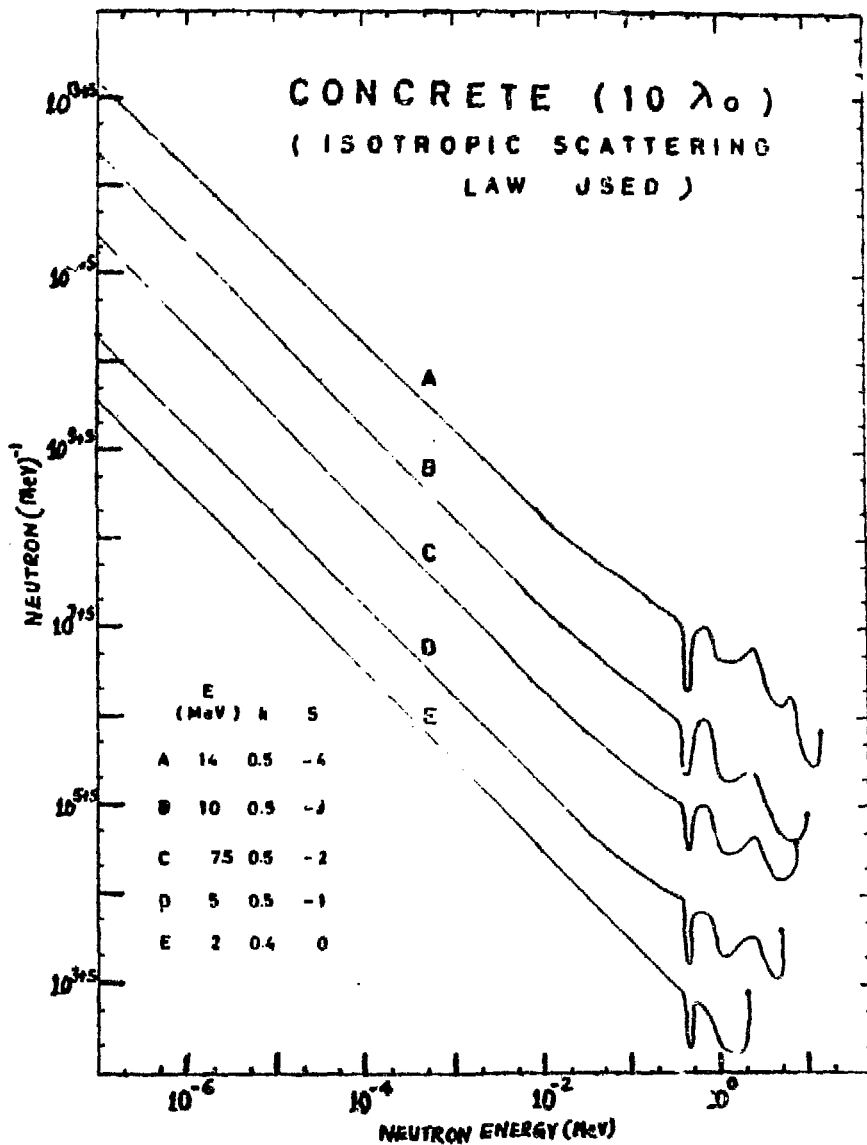


FIG. 7 LEAKAGE NEUTRON SPECTRA THROUGH 10 MEAN FREE PATHS OF CONCRETE

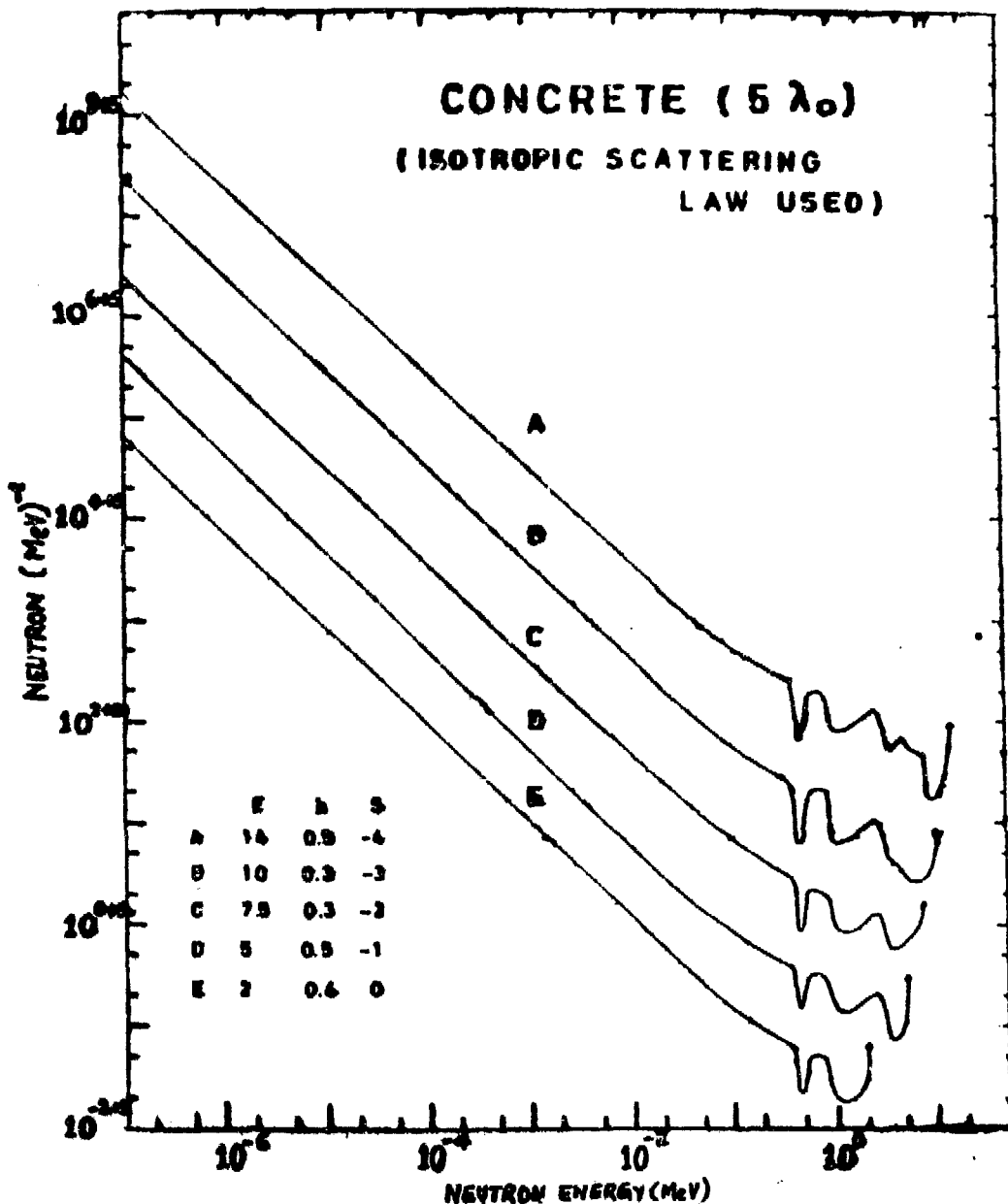


FIG. 5 LEAKAGE NEUTRON SPECTRA THROUGH 5 MEAN FREE PATHS OF CONCRETE

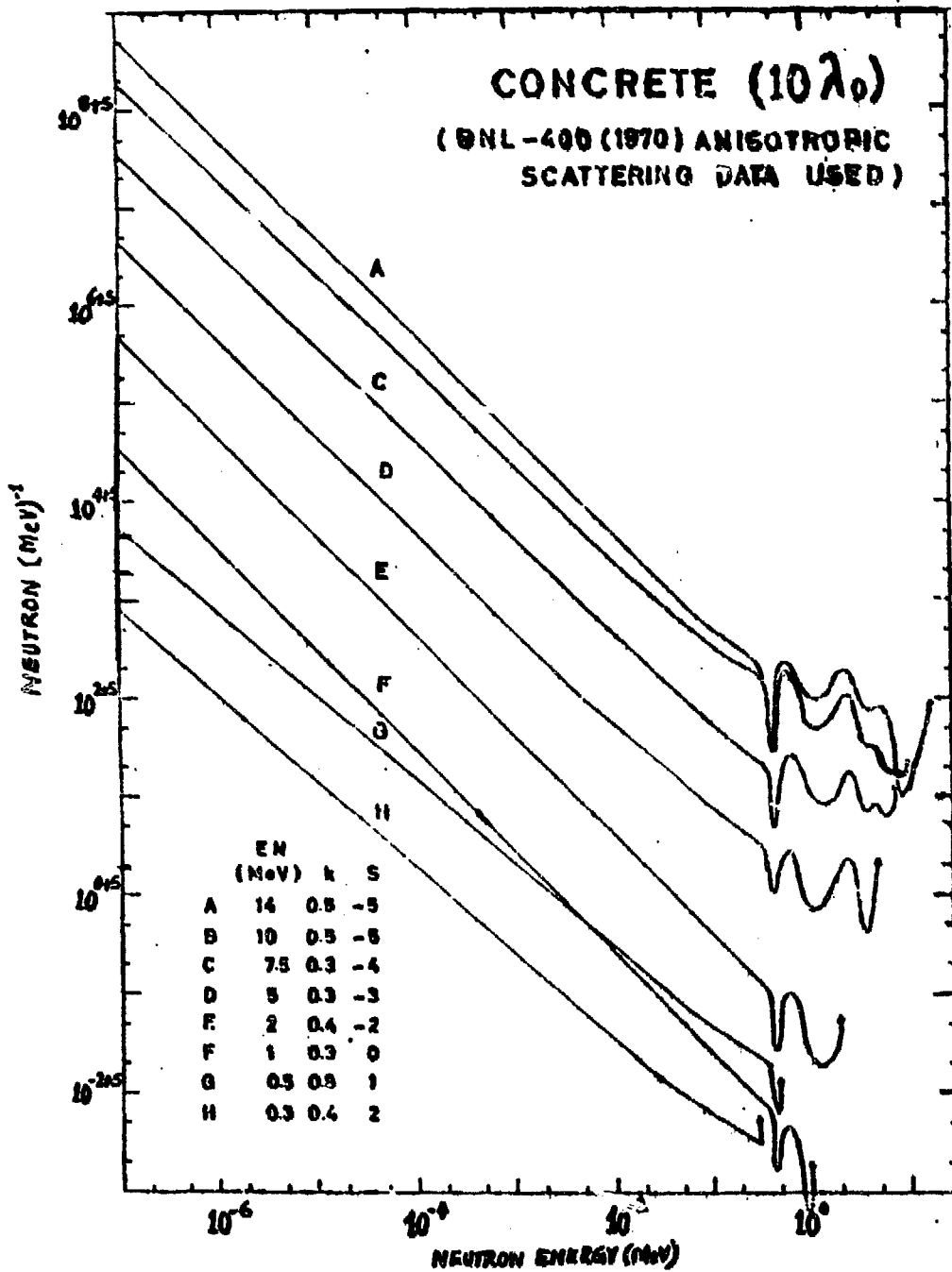


FIG. 8 LEAKAGE NEUTRON SPECTRA THROUGH 10 MEAN FREE PATHS OF CONCRETE

WATER 100cm (ISOTROPIC SCATTERING LAW USED)

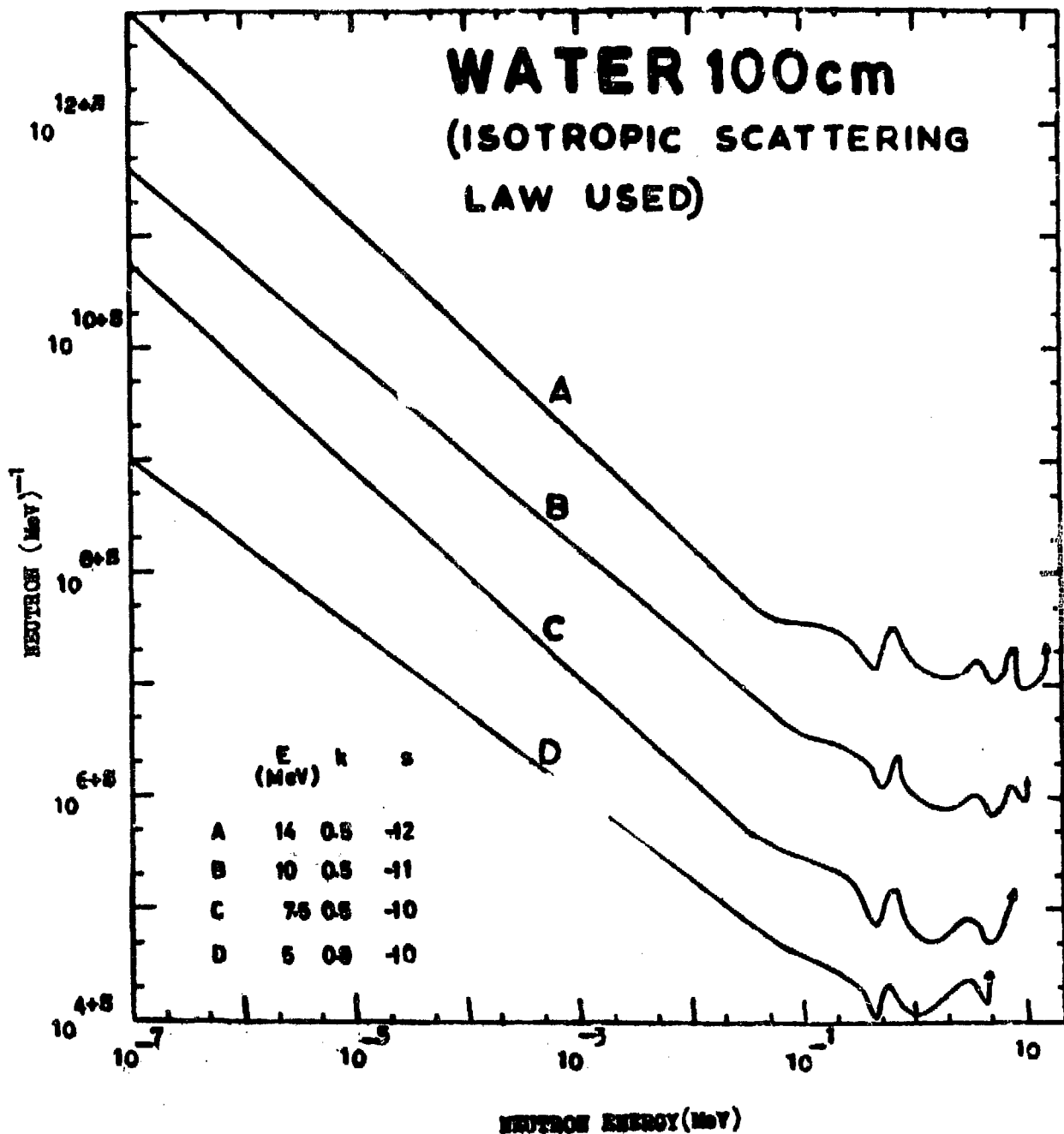


FIG. 9 LEAKAGE NEUTRON SPECTRA THROUGH 100cm OF WATER

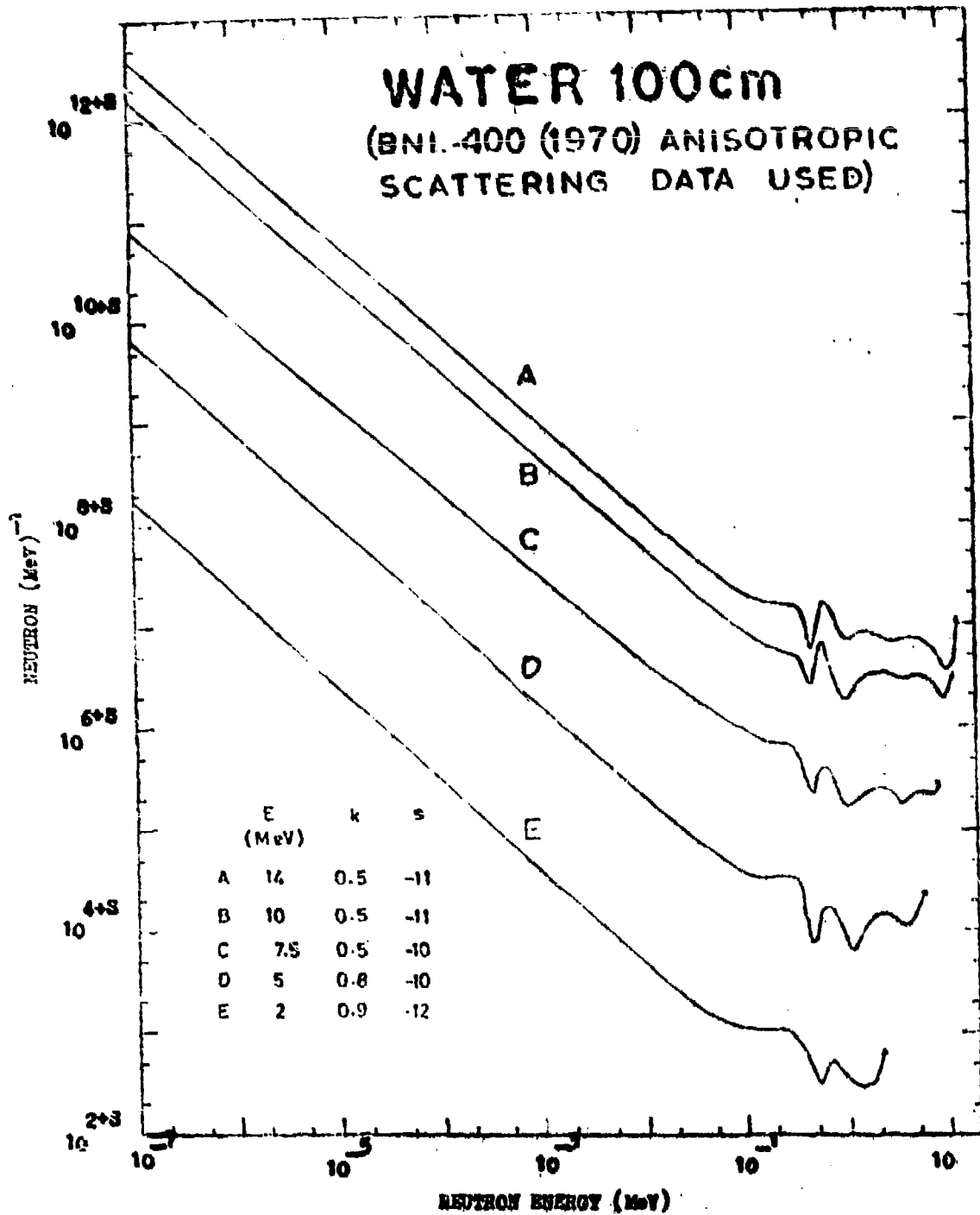


FIG. 10 LEAKAGE NEUTRON SPECTRA THROUGH 100 CM OF WATER

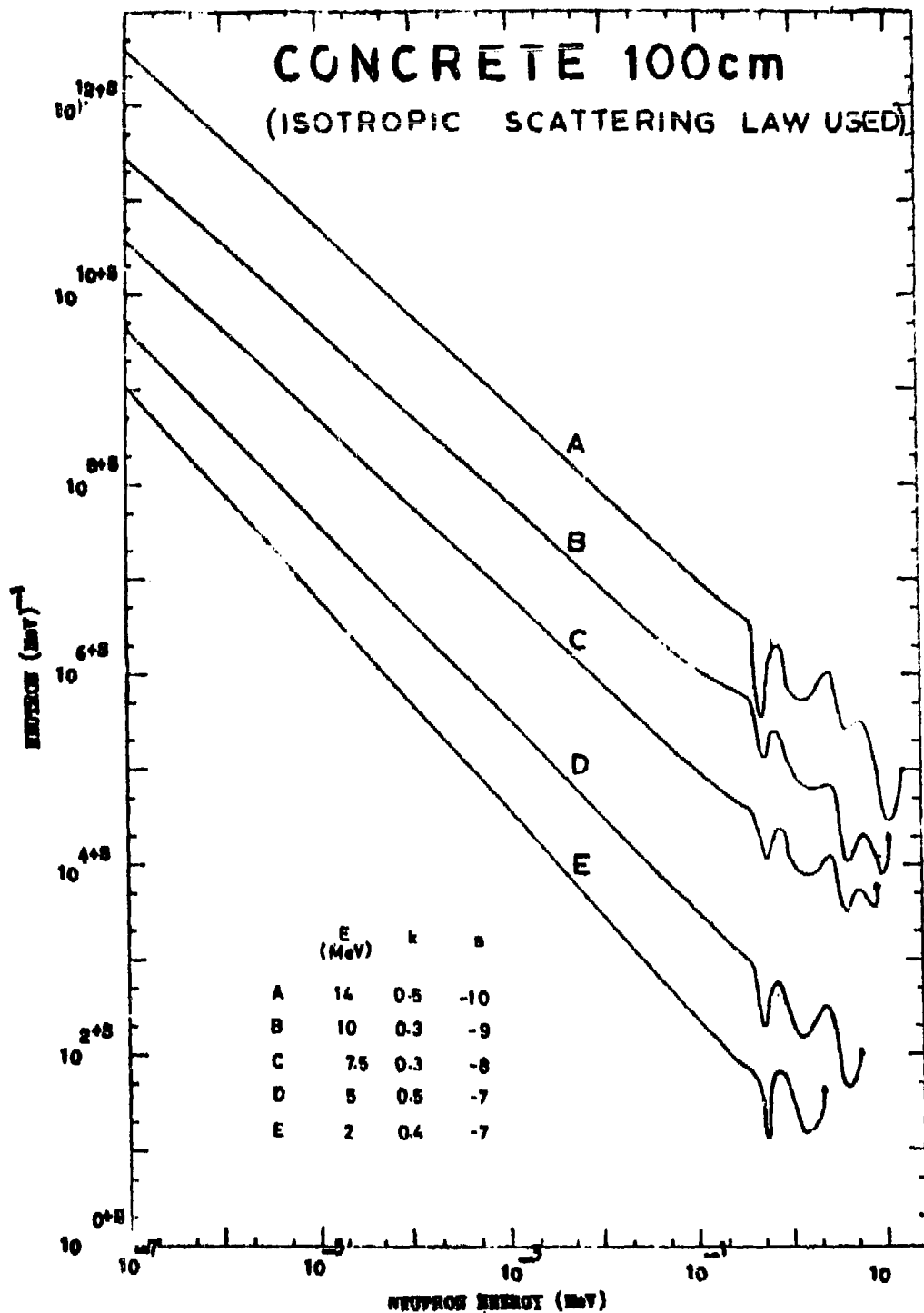


FIG. 11 LEAKAGE NEUTRON SPECTRA THROUGH 100 CM OF CONCRETE

CONCRETE 100cm

(BNL-400 (1970) ANISOTROPIC SCATTERING DATA USED)

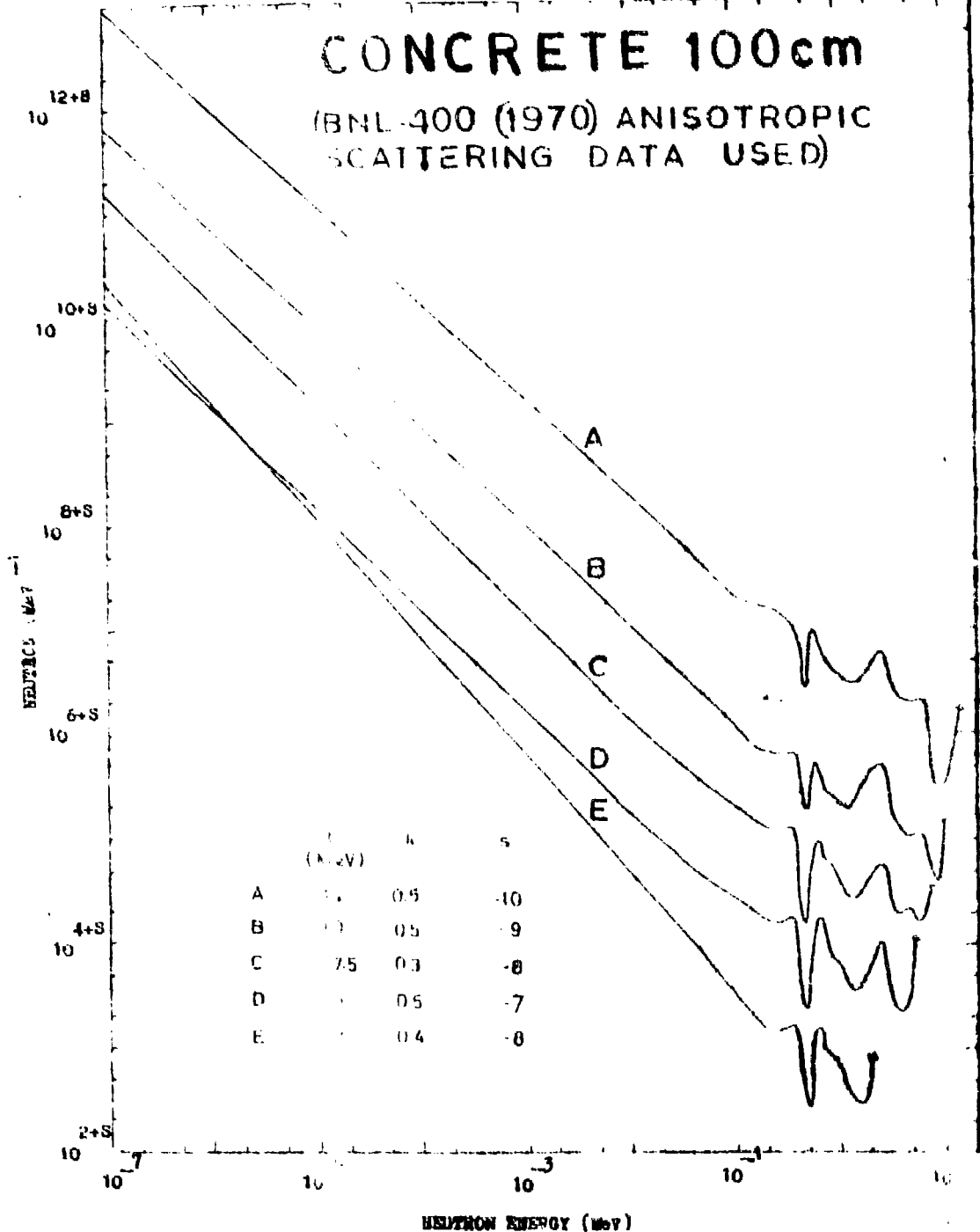


FIG. 12 LEAKAGE NEUTRON SPECTRA THROUGH 100 CM OF CONCRETE

